Available online at www.sciencedirect.com
SCIENCE DIRECT
Polymer 47 (2006) 2750–2759
polymer
www.elsevier.com/locate/polymer

Dilute-solution structure of charged arborescent graft polymer

Seok Il Yun [a,b,*], Robert M. Briber [a], R. Andrew Kee [c], Mario Gauthier [c]

[a] Department of Materials Science and Engineering, University of Maryland, College Park, MD 20742, USA
[b] Condensed Matter Science Division, Oak Ridge National Laboratory, Oak Ridge, TN 37831, USA
[c] Department of Chemistry, Institute for Polymer Research, University of Waterloo, Waterloo, Ont. N2L 3G1, Canada

Received 22 September 2005; received in revised form 7 February 2006; accepted 8 February 2006
Available online 3 March 2006

Abstract

The solutions of charged G1 arborescent polystyrene-*graft*-poly(2-vinylpyridine) copolymers in methanol-*d*4 and D_2O were investigated over a dilute concentration range $\phi = 0.005$–0.05 (ϕ: mass fraction) using small-angle neutron scattering (SANS). Upon addition of acid (HCl) arborescent graft polymers became charged and a peak appeared in SANS data. The interparticle distance (d_{exp}) calculated from a peak position corresponded to the expected value (d_{uni}) for a uniform particle distribution. This indicates the formation of liquid-like ordering due to long-range Coulombic repulsions. The smaller dielectric constant of methanol-*d*4 resulted in long-range electrostatic repulsions persisting to lower polymer concentration than in D_2O. The slow mode scattering was observed by dynamic light scattering measurements for the same polymer solutions, indicating the presence of structural inhomogeneity in the solutions. Both the peak and slow mode disappeared by addition of NaCl or excess HCl into the solutions due to the screening of electrostatic interactions. The G1 polymer grafted with longer P2VP chains ($M_w \sim 30{,}000$ versus 5000 g mol) formed a gel on addition of HCl. This result reveals that molecular expansion is more significant for arborescent polymers with longer ($M_w \sim 30{,}000$) linear polyelectrolyte branches, resulting in gelation for $\phi > 0.01$. Upon addition of NaCl or excess HCl a gel transformed back to a liquid resulted from the screening of electrostatic interactions.

Keywords: SANS; DLS; Dendritic polyelectrolyte

1. Introduction

Arborescent graft polymers are a general class of dendritic polymers such as dendrimers and hyperbranched polymers [1,2]. In contrast to dendrimers, arborescent graft polymers incorporate well-defined linear polymer segments rather than monomers as building blocks, which leads to branched polymers with a cascade-branched structure and very high molecular weights in a few grafting cycles (generations), while maintaining a relatively narrow molecular weight distribution ($M_w/M_n < 1.1$). Dendritic polymers have generated a considerable research interest in nanotechnology because of their controllable dimensions, topology, structure, and chemical functionality on the nanometric scale [3–5]. Charged dendritic polymers are interesting because the recent developments in polymeric nano-applications are increasingly associated with polyelectrolyte system such as biomaterial in aqueous environment and layer by layer structures, etc. [6,7]. The arborescent graft polymers studied in this article is generation 1 (G1), poly(2-vinylpyridine) (P2VP) copolymers where P2VP branches were grafted onto comb-branched polystyrene (G0PS). The poly-(2-vinylpyridine) chains are easily ionized in methanol or water using HCl [8,9]. The charge density of these molecules can be varied by concentration of added HCl. The situation is similar to previously studied PAMAM dendrimers where their terminal amine groups are ionized with HCl and the charge density is controlled by added acid [10–13]. One of the anomalous features of likely charged polymers in solution is the presence of local large-scale structure. Such an inhomogeneity has been confirmed by dynamic light scattering (DLS) measurement [14–20] showing slow dynamics as well as the upturn in a very low q regime by small-angle scattering experiments [20,21]. The two state structure model has suggested that the structural inhomogeneity mentioned above originates from the formation of two phases, disordered (Brownian) regions and highly ordered domains via attractions as well as repulsions [22–27]. According to this model, the observed peak in the small-angle scattering patterns represents ordering within the domains of a higher density, which coexists with less dense

* Corresponding author. Tel.: +1 865 690 4748; fax: +1 865 241 1887.
E-mail address: augustinysi@yahoo.com (S.I. Yun).

0032-3861/$ - see front matter © 2006 Elsevier Ltd. All rights reserved.
doi:10.1016/j.polymer.2006.02.018

disordered regions. Consequently the presence of local inhomogeneity was inferred from the observation that the interparticle distance d_{exp} from the peak position is clearly smaller than expected values, d_{uni} calculated from polyelectrolyte concentration for a uniform particle distribution. The inequality $d_{exp} < d_{uni}$ has been observed as the evidence of the formation of ordered domains for charged colloidal suspensions [24,25] and polyelectrolyte micro-gel solutions [26]. The theory of attraction of likely charged polyelectrolyte solutions causing a two state structure was proposed by Sogami and more recently Schmitz and Bhuiyan [22,23]. The solution structure of charged dendrimers has been examined by several research groups. The charged PAMAM dendrimers were reported to form a two state structure based on the observations of the relationship $d_{exp} < d_{uni}$, for the higher generation ($\geq$G7) [12]. For the relatively low generation dendrimers (G5) of PAMAM and poly(propyleneimine), instead of highly ordered domains, short-range ordering (liquid-like ordering) induced by intermolecular Coulombic repulsions has been proposed for the solution structure [11,13]. The solution properties of neutral (non-charged) arborescent polymers have been extensively studied including P2VP copolymers [28]. To our knowledge no structural investigation has been detailed for arborescent graft polyelectrolyte solutions. The purpose of this article is to investigate the structure of charged arborescent polymers in dilute solution (below an overlap concentration), $\phi = 0.005$–0.05 (ϕ: mass fraction) using SANS and DLS. The main focus is to elucidate the influence of the ionization level, solvent quality and branch size on the structure of arborescent graft polyelectrolyte solutions.

2. Experimental procedures

The synthesis and characterization of the arborescent poly(2-vinylpyridine) copolymers used in this study have been discussed in detail elsewhere [8,9]. The generation 1 (G1) arborescent copolymer molecules used in the investigation was obtained by grafting comb-branched polystyrene (G0PS) substrates with P2VP chains. To study the influence of P2VP chain length on the polyelectrolyte properties, P2VP with a molecular weight of either 5000 (P2VP5K) or 30,000 (P2VP30K) were used as side chains. Since, the molecular weight of arborescent graft polymers grows exponentially for successive generations, the copolymers contained at least 90 mol% P2VP even though the G0 substrate was pure polystyrene. The molecular weight of the side chains was determined by the size exclusion chromatography by analysis of a sample removed from the reactor prior to the grafting reaction. The G0 substrate consisted of a linear polystyrene backbone ($M_w = 5420$, $M_w/M_n = 1.09$) grafted with 12 polystyrene side chains ($M_w = 5220$, $M_w/M_n = 1.07$), for a total $M_w = 6.7 \times 10^4$ as shown in Table 1. The characteristics of copolymers are given in Table 2.

Table 1
Characteristics of arborescent polystyrene substrates

Generation	Branches		Graft polymers	
	M_w (g mol^{-1}) (SEC)[a]	M_w/M_n (SEC)[a]	M_w (LS)[b] (g mol^{-1})	f_w (tot)
G0PS	5220	1.07	6.7×10^4	12

[a] Values from SEC analysis using linear PS standards calibration.
[b] Absolute M_w of the graft polymers from laser light scattering.

Deuterated methanol (CD_3OD, methanol-$d4$) and deuterium oxide (D_2O) were used as solvents. Methanol-$d4$ was a good solvent for the G0PS-P2VP copolymers and HCl was added to the solutions to charge the polymers. The copolymers would not dissolve in D_2O until HCl was added. Each 2VP unit carries one aromatic amine functionality that can be ionized upon addition of HCl. The charge density is defined as the stoichiometric ratio of added HCl to the total number of amine groups in the polymer solution (Eq. (1)). When α is equal to 1, all the 2VP units are assumed to be ionized.

$$\alpha = \frac{\text{moles HCl}}{\text{moles P2VP}} \tag{1}$$

Small-angle neutron scattering (SANS) experiments were carried out at the Center for Neutron Research at the National Institute of Standards and Technology on the 30 m NIST-NG3 and NG7 instruments [29,30]. The raw data were corrected for scattering from the empty cell, incoherent scattering, detector dark current, detector sensitivity, sample transmission, and thickness. Following these corrections the data were placed on an absolute scale using either a calibrated secondary standard or direct beam measurement and circularly averaged to produce $I(q)$ versus q plots where $I(q)$ is the scattered intensity and q is the scattering vector ($q = \sin\theta 4\pi/\lambda$). The q range was 0.0046–0.0820 Å^{-1} and the neutron wavelength was $\lambda = 6$ Å with a wavelength spread $\Delta\lambda/\lambda = 0.15$.

Dynamic light scattering measurement was carried out using a Malvern Zetasizer 3000. Photon autocorrelation functions were obtained from a Malvern 7132 correlator at an angle 90°. The laser used for this wok is a nominal 5 mW helium neon continuous power model having a wavelength 633 nm. Sample temperature was maintained 25°C. For dynamic scattering the real time random motion of polymer in solution is considered. The instantaneous scattering intensity $I(q, t')$ at time t' correlates the intensity after an elapsed time τ (at time $t' + \tau$). This correlation is defined by the autocorrelation function, $G(\tau)$ [31].

$$G(\tau) = \langle I(q,0) I(q,\tau) \rangle = \lim_{t \to 0} \left[\frac{1}{t} \int_0^t I(q,t') I(q,t'+\tau) dt' \right] \tag{2}$$

When $\tau = 0$, the autocorrelation function is $\langle [I(q,0)]^2 \rangle$, the mean-square value of the intensity. For the Brownian motion of a monodisperse solute, the decay curve is that of a single exponential and

$$G(\tau) = \langle I(q,0) \rangle^2 + \left[\langle [I(q,0)]^2 \rangle - \langle I(q,0) \rangle^2 \right] \exp\left(-\frac{\tau}{\Gamma}\right) \tag{3}$$

Table 2
Characteristics of arborescent 2-vinylpyridine graft copolymers

Copolymers	Side chains		Graft polymer composition/mol% P2VP[c]	Graft copolymers	
	M_w (g mol$^{-1)}$ (SEC)[a]	M_w/M_n (SEC)[a]		M_w (g mol^{-1}) (LS)[b]	f_w(tot)
G0PS-P2VP5K	5820	1.08	90	7.2×10^5	112
G0PS-P2VP30K	28,600	1.09	97	3.2×10^6	111

[a] Values from SEC analysis using linear PS standards calibration.
[b] Absolute M_w of the graft polymers from laser light scattering.
[c] Copolymer composition determined using ^{1}H NMR spectroscopy.

where $\Gamma = 1/2q^2D$ and D is the diffusion coefficient. D was determined by fitting autocorrelation function to the following simple expression with three fitting parameters, the amplitude A, the base line B and the D

$$G(\tau) = \left[A\exp\left(-q^2D\tau\right)\right]^2 + B \quad (4)$$

The hydrodynamic radius R_h of the particles was obtained using the Stokes–Einstein equation:

$$D = kT/6\pi\beta R_h \quad (5)$$

where k is the Boltzmann constant, T is the absolute temperature, β is the solvent viscosity.

The correlation curves were analyzed for the multimodal distribution of particles in solution using the CONTIN algorithm written by Provencher [32].

3. Results and discussion

Fig. 1(a) shows SANS data collected for G0PS-P2VP5K copolymer in methanol-*d*4 in which polymer concentration is fixed at $\phi = 0.03$ and α was varied from 0.0 to 0.3. The progressive decrease of the scattering intensity in very low q correlates well with the increase of the total osmotic pressure upon increasing acid concentration. The most notable effect upon addition of acid is the appearance of a scattering peak, which is a common feature for polyelectrolyte solutions and is consistent with the previous observations of dendritic polyelectrolyte solutions [10–13]. The origin of the peak has been normally interpreted for dendritic polyelectrolyte solutions as a correlation peak of which position is related to an inter-particle distance due to long-range Coulombic interactions. As provided in Fig. 1(a) the peak becomes more pronounced with its increasing charge density up to $\alpha = 0.3$, showing that ordering is enhanced owing to the increasing number of ionized 2VP monomers. The location of the peak is roughly maintained unchanged as a function of α. The origin of the peak in the scattering curve can be further understood by examining the dependence of the peak position on polymer concentration. The SANS curves for G0PS-P2VP5K (ionized with $\alpha = 0.5$) molecules in methanol-*d*4 are shown as a function of polymer concentration in Fig. 1(b). The location (q^*) of the peak moves to higher q as ϕ increases following the scaling law $q^* = k\phi^n$ with $n = 0.313 \pm 0.01$ which corresponds to a simple volume expansion ($n = 1/3$) of the interparticle distance with decreasing polymer concentration. A scaling exponent of about 1/3 has been reported for spherical polyelectrolyte systems such as charged dendrimers [10–13], micelles [33], and globular biopolymer solutions [34]. The nearest neighbor interparticle distance d_{exp} was estimated from the observed q^* and compared with the average interparticle distance d_{uni} calculated from the molecular weight and polymer concentration assuming a face-centered-cubic (FCC) lattice and simple-cubic (SC) lattice (Table 3). For an FCC lattice, the nearest neighbor interparticle distance is given by

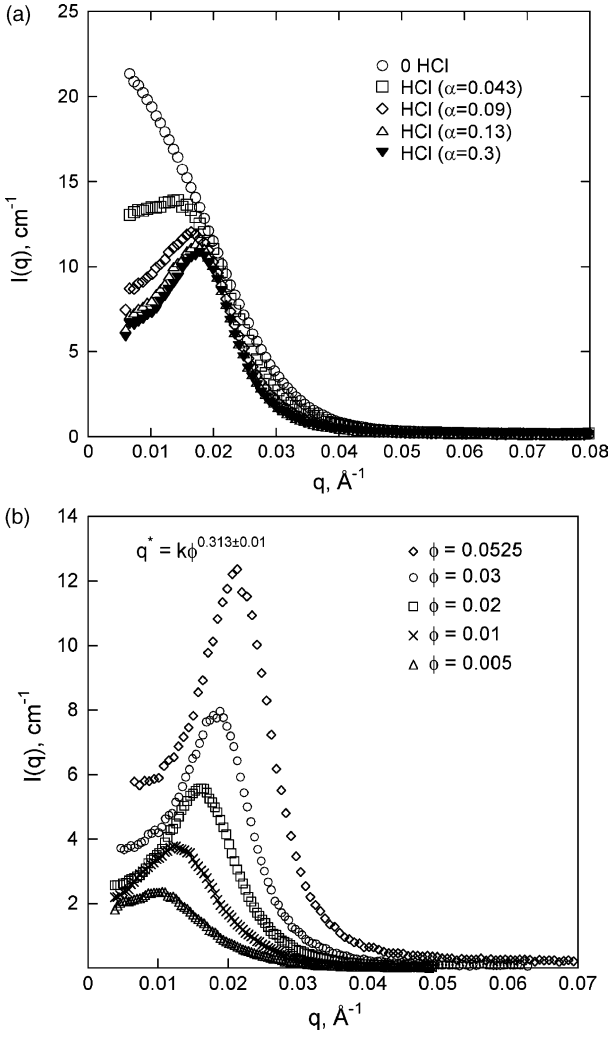

Fig. 1. SANS data of G0PS-P2VP5K in methanol-*d*4 (a) ($\phi = 0.0313$) as a function of acid concentration, α (b) ($\alpha = 0.4$) as a function of polymer concentration, ϕ.

$d_{exp} = \sqrt{6}\pi/q^*_{(111)}$, where q^* is the (111) peak position. The nearest average interparticle distance d_{uni} was calculated from

$$d_{uni} = \frac{\sqrt{2}}{2}\left(\frac{4M_w}{N_A C_m}\right)^{1/3} \quad (6)$$

where M_w is the molecular weight, N_A is Avogadro's number and C_m is the mass concentration. For a simple cubic lattice, $d_{exp} = 2\pi/q^*_{(100)}$ and the nearest average interparticle distance was calculated using

$$d_{uni} = \left(\frac{M_w}{N_A C_m}\right)^{1/3} \quad (7)$$

The results summarized in Table 3 show that the values of d_{exp} agree with (for FCC, slightly larger than) d_{uni} for all concentrations investigated confirming the absence of inequality, $d_{exp} < d_{uni}$ which has often been observed for charged colloidal systems [24–26]. The relationship $d_{exp} \cong d_{uni}$ suggests that the peak originates from the liquid-like ordering of likely charged arborescent graft polymers that uniformly correlate throughout the solution. For ordinary non-charged molecular fluids, the high packing density, the volume fraction $\eta = 0.3$–0.5 is necessary to produce liquid-like ordering induced by short-range repulsive potentials. In contrast, charged colloidal suspensions correlate via long-range Coulombic interactions and liquid-like ordering normally occurs at packing densities as low as $\eta = 0.001$. The observed liquid-like ordering for the arborescent graft polyelectrolyte solutions at very low concentration $\phi = 0.005$ indicates the strong influence of long-range electrostatic interactions on the solution structure. The liquid-like ordering has also been observed for charged dendrimer solutions [11,13]. Recent experimental studies confirm that the size of dendrimers remains unchanged upon charging them [11,35]. This result clearly shows that the liquid-like ordering of dendrimer polyelectrolyte solutions is not caused by the hard sphere interaction of expanded dendrimers, but by purely long-range electrostatic repulsions. The size expansion for charged arborescent polymers is found to be larger than dendrimer but relatively insignificant for polymers grafted with short branch of 5K [9]. The peak was seen in the SANS curves for charged G0PS-P2VP5K copolymers at low concentration $\phi = 0.005$ where the interparticle distance is significantly greater than the particle diameter of charged molecules. In the previous SANS investigation for non-charged G0PS-P2VP5K polymers, we demonstrated that the peak was not found even at high concentration $\phi = 0.053$ where the polymers are close to an overlap condition [28]. These reveal that liquid-like ordering (peak) originates from long-range electrostatic interactions for charged arborescent polymers in solution.

The combined investigation of SANS with DLS measurements was carried out for charged solutions. The results by both SANS and DLS measurements for G0PS-P2VP5K copolymers at $\phi = 0.005$ as a function of α are provided in Fig. 2. As shown in Fig. 2(a) the peak in the SANS patterns disappears upon addition of HCl in excess of the stoichiometric amount ($\alpha > 1$) where all 2VP are already ionized and further added acid increases counterion concentration, leading to the screening of electrostatic interactions. The radius of gyration (R_g) was calculated using Guinier's equation, $I(q) = I(0)\exp\left(-R_g^2 q^2/3\right)$. The R_g values for uncharged and fully screened G0PS-P2VP5K molecules are nearly equivalent. The scattering becomes eventually similar to that of uncharged polymer solution although the scattering intensity of fully screened solutions remains smaller than that of neutral polymer. The diffusion distribution curves obtained by DLS for G0PS-P2VP5K copolymer at $\phi = 0.005$ in methanol are shown in Fig. 2(b). Upon addition of HCl one average diffusive relaxation split into two modes in the diffusion distribution curves. The solution of neutral polymer with a narrow polydispersity typically shows one average diffusive relaxation by DLS. However DLS auto correlation function for polyelectrolyte solutions normally show two exponential decay times yielding to two diffusive relaxations, faster and slower than that of the corresponding neutral polymer solution. This anomalous dynamic behavior of polyelectrolyte solutions was termed the ordinary–extraordinary transition. A slow mode

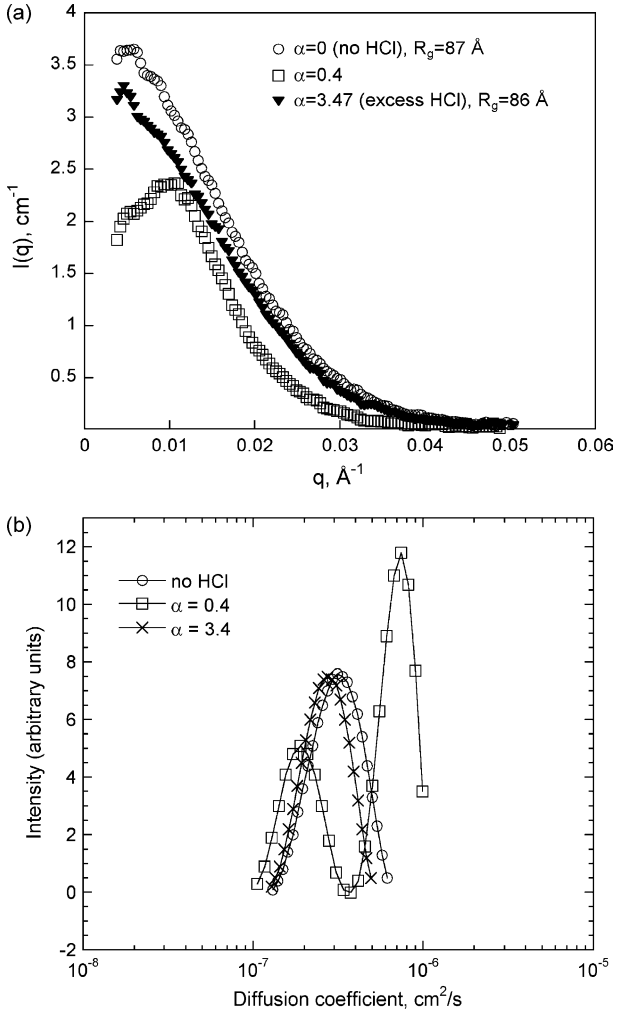

Fig. 2. Comparison of SANS and DLS measurement of G0PS-P2VP5K with different acid concentration α at the same polymer concentration $\phi = 0.005$ (a) SANS data as a function of α in methanol-*d*4 (b) diffusion distribution curves as a function of α in methanol.

has been reported for nearly all types of polyelectrolyte systems including colloidal suspensions and charged dendrimers [14,15]. Although the low q upturn was not clearly seen in the SANS patterns for charged G0PS-P2VP5K polymer solutions, the slow mode observed by DLS in Fig. 2(b) possibly indicates the presence of local large-scale structures in the solutions. However, the observed slow mode is only two times smaller compared to the single mode from the neutral arborescent polymer solutions, while the separation between the slow mode and the single mode of the corresponding neutral polymer has been found to be at least one order of magnitude for the most of linear polyelectrolyte and charged colloidal systems. The Fig. 3(a) shows the auto correlation function with increasing polymer concentration. At higher ϕ, the double exponential of correlation function becomes more evident compared to lower concentration solutions resulting in the decrease of the slow mode as a function of ϕ as shown in Fig. 3(b). Another interesting feature of DLS measurements is that two modes merge back into a single mode, recovering the dynamics of neutral polymer solutions upon addition of stoichiometric excess HCl ($\alpha > 1$) due to the screening of electrostatic interactions. Some studies proposed that structural

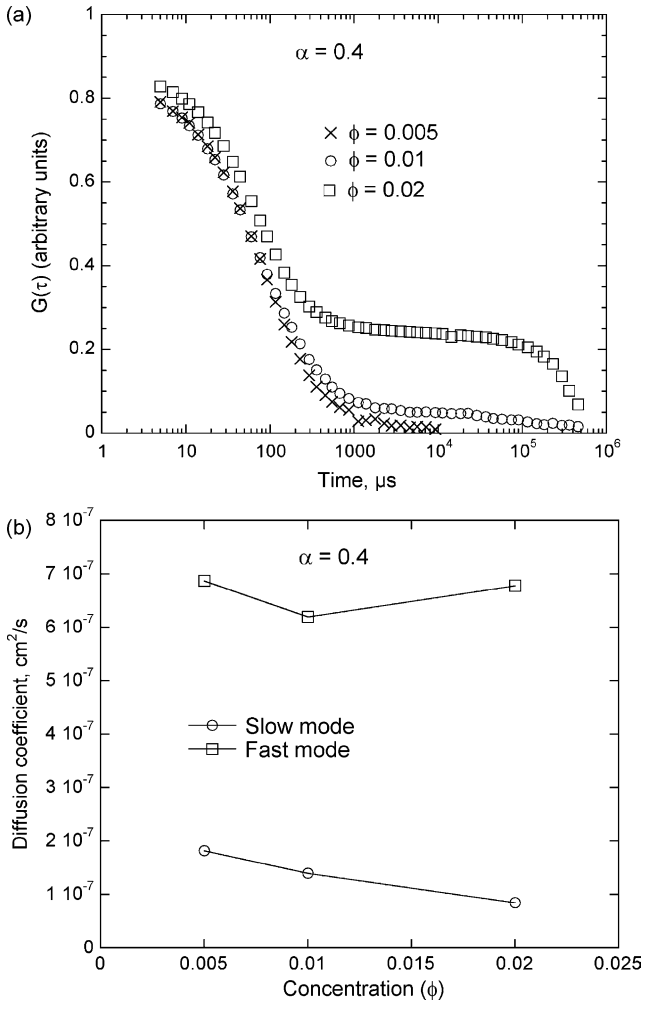

Fig. 3. (a) Auto correlation function as a function of ϕ (b) diffusion coefficient of the fast and slow mode as a function of ϕ.

inhomogeneity is due to the macroscopic demixing promoted by hydrophobic interactions of backbone [36,37]. The disappearance of the slow mode by screening effect, however, indicates that inhomogeneity does not result from hydrophobic G0 polystyrene comb but by purely electrostatic interaction. The average diffusion coefficient for the uncharged and fully screened polymer is nearly identical agreeing with the R_g measurement by SANS (Fig. 2(a)). The fast mode has been explained in terms of polyion-counter ion coupling. The fast diffusion mode shown in Fig. 3(b) is essentially found to be independent of concentration agreeing with some other experimental results [16–18].

The considerable research efforts have been made to account for the coexistence of local inhomogeneity and ordering in polyelectrolyte solutions, although currently no theory is widely accepted by polymer science community. The low q upturn was previously observed for dendrimer polyelectrolyte solutions and interpreted as the indicative of local large-scale structures, possibly aggregates in the solutions which exhibit liquid-like ordering at the same time. Similarly the slow dynamics for arborescent polyelectrolyte solutions could be attributed to the formation of temporal aggregates, which are floating in liquid-like ordering phase. This interpretation is analogous to the structural analysis for linear polyelectrolyte solution by Förster showing that temporal aggregates freely move in semi-dilute net work structure in the solutions [17]. Assuming that the slow mode originated from the dynamics of aggregates in the arborescent polyelectrolyte solutions, the structure of aggregates should have been well resolved by SANS within the q range investigated, given the relatively small size of the slow mode calculated by Eq. (5). Such a low q scattering, however, has not been seen in SANS data. It is then possible to infer that the slow mode by DLS does not represent aggregates but some other kind of local inhomogeneity. One of the interesting results drawn from the combined investigation of DLS with SANS is that the screening of electrostatic interactions eliminates not only the slow mode but also the peak in SANS data as shown in Fig. 2. This behavior may imply that local inhomogeneity and liquid-like ordering possibly originate from the same Coulombic repulsions. This argument is also conceptually similar to the model proposed by Ermi et al. in the aspect that ordering and the aggregation have same origin, which is however, an attraction for the case of linear polyelectrolyte system [38]. For arborescent polyelectrolyte, the idea of the same origin for both ordering and structural inhomogeneity in the solution may not favor 'attraction' but rather 'repulsion' for the origin of inhomogeneity. The aggregation and a two state structure model are based on the same concept that the attraction is responsible for structural inhomogeneity. Besides the attraction of likely charged macroions, Roji et al. suggested that charged colloidal particles undergo a fluid–fluid (gas–liquid) phase separation although they interact via a purely repulsion. This indicates that attraction is not necessary for local inhomogeneity in polyelectrolyte solutions [39]. However, even in the case of a fluid–fluid (gas–liquid) phase separation by repulsions for arborescent graft polyelectrolyte solutions, the absence of

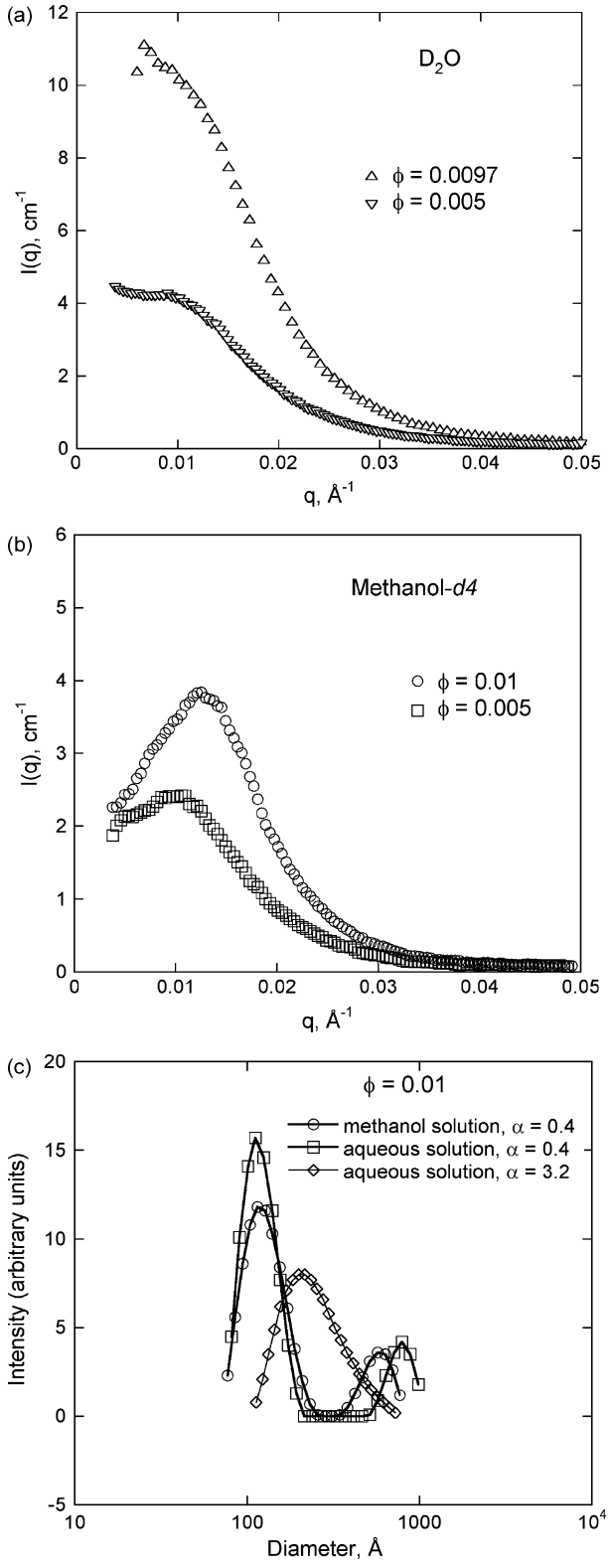

Fig. 4. Comparison of SANS data of charged G0PS-P2VP5K for very dilute concentration $\phi \leq 0.01$ in (a) D_2O and (b) methanol-*d*4. DLS measurement (c) Particle diameter distribution curves at $\phi = 0.01$.

the low scattering or upturn in the SANS data for arborescent polyelectrolyte solutions is still a question. We tentatively conclude that the origin of the slow mode by DLS may be related to temporarily correlated movements of a few charged molecules or branches within liquid-like ordering rather than a separated phase.

Table 3
Comparison of d_{exp} and d_{uni} for G0PS-P2VP5K in methanol-*d*4

ϕ	Simple cubic		Face-centered cubic	
	d_{exp} (Å)	d_{uni} (Å)	d_{exp} (Å)	d_{uni} (Å)
0.005	595	598	729	671
0.010	501	477	613	536
0.020	390	376	477	422
0.030	333	328	408	369
0.053	299	295	366	331

The screened Coulombic repulsions of spherical electrolyte can be described by the classical DLVO (Derjaguin–Landau–Verwey–Overbeek) theory. Ignoring the weak van der Waals contribution to the DLVO potential, the repulsive potential between two identical spherical macroions of diameter σ is [40]

$$U(r) = \pi\varepsilon_0\varepsilon\sigma^2\psi_0^2\exp\left(-\frac{r-\sigma}{k}\right)/r, \quad r > \sigma \tag{8}$$

where r is the interionic center-to-centre distance, ψ_0 is the surface potential, ε is the dielectric constant of the solvent medium, and ε_0 is the permittivity of free space. κ is the Debye-Hückel screening length determined by the ionic strength of the solution and $\kappa^2 = 4\pi l_B \mu$ ($l_B = Q^2/\varepsilon k_B T$ is the Bjerrum length, μ is the ionic strength and T is the temperature). The SANS data of charged arborescent polymers in D_2O and methanol-*d*4 at low ϕ ($\phi \leq 0.01$) are compared in Fig. 4. The DLVO theory predicts that the kind of solvent should have a significant effect on the strength and the range of electrostatic interaction due to the different ε. The screening length κ is inversely proportional to the square root of the dielectric constant of the solvent. As a result Coulombic interactions should be more effectively screened in D_2O ($\varepsilon = 80$) than in methanol-*d*4 ($\varepsilon = 36$). No clear scattering peak was observed in D_2O solutions at these low concentrations (only a weak shoulder is visible in the $\phi = 0.005$ sample), consistent with more effective screening of electrostatic interactions because of the higher value of ε. A peak is discernable in D_2O for slightly higher concentration, $\phi = 0.0102$ compared to 0.0096. The scaling factor for $q^* \sim \phi^n$ in D_2O is found to be $n = 0.377 \pm 0.034$. The d_{exp} values for polymers in D_2O agree with (for FCC, slightly larger than) the d_{uni} showing that charged arborescent polymers form liquid-like ordering in the aqueous solution as well as in methanol. The d_{exp} values estimated from the observed q^* in D_2O is slightly smaller than in methanol-*d*4 as given in Tables 3 and 4. The DLS measurements were carried out on the aqueous solutions of the charged arborescent polymers. Similar to the

Table 4
Comparison of d_{exp} and d_{uni} for G0PS-P2VP5K in D_2O

ϕ	Simple cubic		Face-centered cubic	
	d_{exp} (Å)	d_{uni} (Å)	d_{exp} (Å)	d_{uni} (Å)
0.0102	485	477	594	536
0.0200	367	376	450	422
0.0300	327	328	401	369

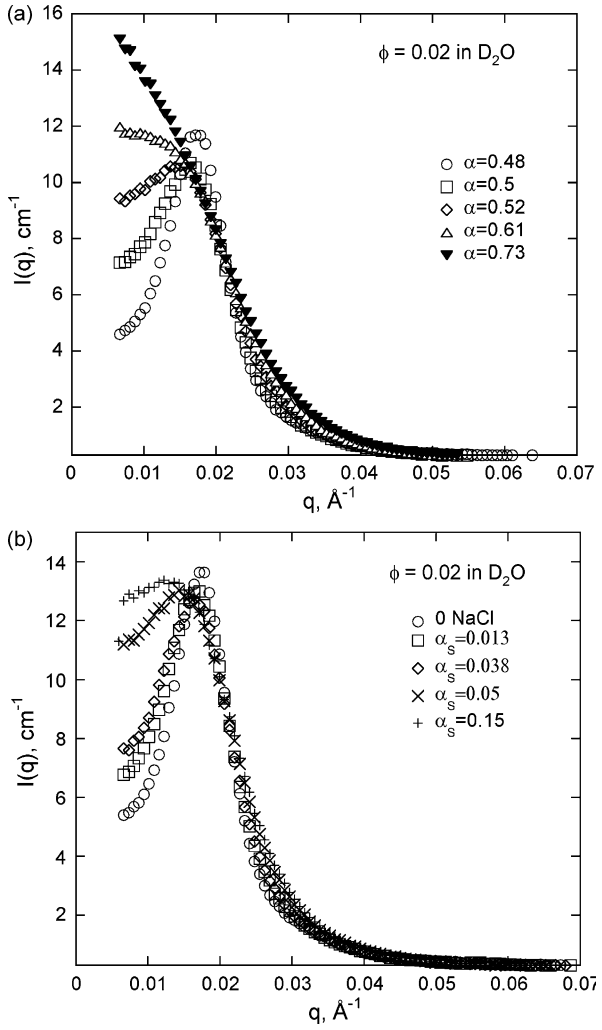

Fig. 5. SANS data for charged G0PS-P2VP5K at $\phi = 0.02$ in D_2O (a) as a function of α (b) as a function of NaCl concentration, α_S.

solutions in methanol, DLS of the aqueous solutions shows the slow and fast mode which are to merge back to a single mode upon addition of stoichiometric excess HCl due to the screening of electrostatic interactions (Fig. 4(c)). The R_h value from the slow mode in water by Eq. (5) is slightly larger than in methanol, while the value of R_h for the fast mode does not change in both solutions under the same concentration.

Fig. 5(a) provides the SANS data for G0PS-P2VP5K copolymers in D_2O in which polymer concentration is fixed at $\phi = 0.03$ and α was varied from 0.48 to 0.78. The SANS data of neutral solution is not available because G0PS-P2VP5K copolymer dissolves in water only upon addition of HCl. The G0PS-P2VP5K copolymers in D_2O at $\alpha = 0.48$ exhibit the peak in the SANS patterns. Interestingly the polyelectrolyte peak vanishes upon the further addition of HCl ($\alpha > 0.48$) and no peak was observed at $\alpha \sim 1$ where the charge density is expected to maximize. This result is different from charged PAMAM dendrimer solutions which showed the most pronounced peak at $\alpha = 1$ by SANS [11]. The arborescent polymer is highly branched polymer and the charge density of its polyelectrolyte is much higher than dendrimer polyelectrolytes. For instance, the total number of potentially ionized sites at $\alpha = 0.4$ for the G1 polymer studied here is 2200 which is substantially larger than 128 terminal amine groups of the G5 PAMAM dendrimers [11]. The polyelectrolyte theory for highly branched polymer solution predicts that most of the counterions are drawn into within polymer intrachain volume even in dilute solutions (charge renormalization). Consequently the effective charge becomes substantially small and the interaction of polyelectrolyte is governed by the entropic contribution of the trapped counterions instead of electrostatic interactions, termed osmotic behavior [41,42]. No peak in the SANS data indicates that most of counterions condensed into the strongly charged arborescent polymer ($\alpha \sim 1$). Based on the gradual diminishment of the polyelectrolyte peak in the regime $0.5 < \alpha < 1$, the transition from an electrostatic to osmotic regime (fully screened) occurs gradually as a function of α. The transition regime $0.5 < \alpha < 1$ can be considered an intermediate regime where the electrostatic repulsions between molecules is still strong enough to exhibit the interference peak, showing incomplete charge renormalization. The observed intermediate regime is more complex compared with some theories which assume either purely osmotic (fully screened) or purely electrostatic regimes depending on the charge density [42]. The screening of Coulombic interactions in acid solutions can also be achieved by adding the salt. The neutralization degree, α_S is defined as the stoichiometric ratio of added salt to the number of protons added in acidic solutions given by

$$\alpha_S = \frac{\text{moles HCl}}{\text{moles NaCl}} \tag{9}$$

The scattering curves of G0PS-P2VP5K copolymer at $\phi = 0.03$ in D_2O are shown in Fig. 5(b) as a function of α_S. The ionization degree is fixed at $\alpha = 0.48$, but added salt concentrations varied from $\alpha_S = 0.01$ to 0.15. Similar to the screening observed in the intermediate regime by excess [43] HCl ($\alpha > 0.48$), the polyelectrolyte peak gradually diminishes with increasing α_S.

According to the Hayter and Penfold model, the surface potential ψ_0 in Eq. (8) is related to the charge number z on the macroion by

$$\psi_0 = \frac{z}{\pi\varepsilon_0\sigma(2 + k^{-1}\sigma)} \tag{10}$$

The scattering intensity is given by the product of the structure factor $S(q)$ and the particle form factor $P(q)$:

$$I(q) = n_p P(q) S(q) \tag{11}$$

where n_p is the particle number density. The structure factor, $S(q)$ for the DLVO potential (Eq. (8)) was calculated by Hayter and Penfold using a mean spherical approximation [40]. Combining $P(q)$ of a hard sphere model and $S(q)$ by the Hayter and Penfold model, the scattered intensity for spherical polyelectrolyte such as charged G0PS-P2VP5K copolymers can be calculated. This model was used to fit the SANS data for charged G0PS-P2VP5K copolymers in D_2O ($\phi = 0.02$) and the best fits are provided in Fig. 6(a). The adjustable parameters were the molecular diameter (σ), volume fraction (η) of the

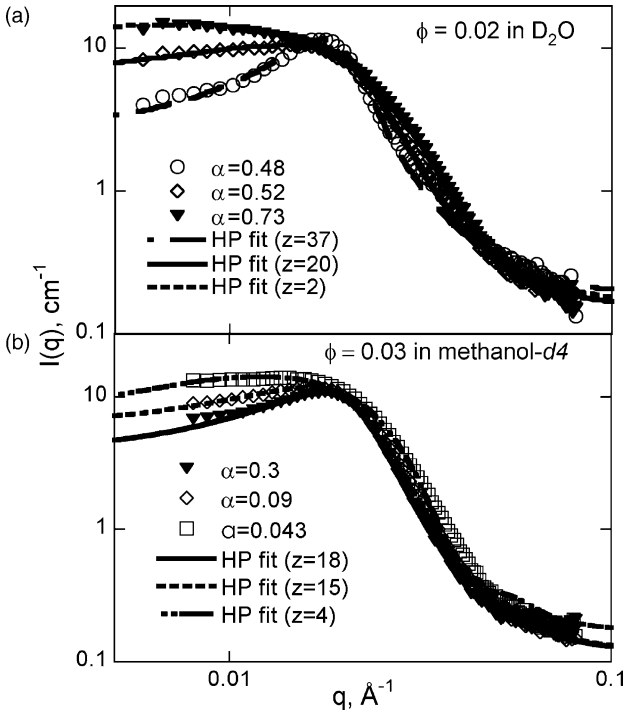

Fig. 6. Hayter–Penfold (HP) model fits to SANS data of G0PS-P2VP5K as a function of α in (a) D_2O ($\phi=0.02$) (b) methanol-$d4$ ($\phi=0.03$).

polyelectrolyte, excess salt concentration (C_s), and the charge number (z). The charges were assumed to be monovalent. The Schulz distribution was used to describe the polydispersity. The validity of the parameters determined by fitting can be examined by the following relation [28]

$$\eta = C\frac{(\sigma/2)^3}{\left(\frac{3M_w}{4\pi N_A d}\right)} \tag{12}$$

where d is the density of polymer, η is the volume fraction of swollen polyelectrolyte dissolved in the solution and C is the volume fraction of (dry) polymer. The η and σ values obtained from the fits in Fig. 6(a) correlated well with polymer concentration (C) and molecular weight via Eq. (12). The quality of the fit to the experimental data, particularly the peak region was sensitive to the change in the charge number (z). The molecular diameter σ from the fits roughly remain constant about 166 ± 8 Å as a function of α. Since, no excess HCl was added ($\alpha<1$), a fitting parameter C_s was fixed at zero. The number of charges per molecule attained from the fits decreases with increasing α, which is consistent with the gradual diminishment of the scattering peak. Fig. 6(b) shows the best fits to the experimental data for charged G0PS-P2VP5K polymers in methanol-$d4$ in the regime $\alpha=0.043$–0.3, where the peak becomes sharper with increasing α. The number of charges per molecule from the fit increases as a function of α, which is consistent with the progressive development of the scattering peak. Using the Hayter–Penfold model for $S(q)$ clearly demonstrated the strong correlation between the peak development and the effective charge number of molecules, in other words, long-range Coulombic repulsions. The DLVO potential by the Hayter–Penfold model, qualitatively describes well intermolecular long-range Coulombic repulsions which generated the liquid like ordering of arborescent graft polyelectrolyte solutions, however, the model does not account for some of the key features of highly branched polyelectrolyte systems. The Hayter–Penfold model assumes that the charge is only on the surface of spheres while for arborescent graft polyelectrolytes the ionization of 2VP units can occur throughout the molecule. Furthermore, the model also does not take into account the effects of strong charge renormalization of highly branched polyelectrolyte, osmotic pressure upon addition of acid to the solutions and structural inhomogeneity. The quantitative results from the fitting may be unrealistic (for example at $\alpha=0.4$ the number of ionized sites was estimated to be 37 from the fit, as compared with the presence of $\sim$2200 potential ionizable groups). Regardless of some drawbacks of the model, the variation of z value obtained from the fits by the Hayter–Penfold model qualitatively follows well the trend of the peak evolution as a function of charge density.

To examine the influence of P2VP chain length on the polyelectrolyte behavior, SANS was performed on 30K P2VP polymer (G0PS-P2VP30K) for a comparison with 5K polymer (G0PS-P2VP5K) discussed up to now. The viscosity of G0PS-P2VP30K copolymer in methanol-$d4$ increases dramatically as a function of α. At $\phi=0.01$ G0PS-P2VP30K copolymer solution immediately forms a gel on addition of HCl for $0<\alpha<0.4$. The formation of a gel at $\phi=0.01$ for G0PS-P2VP30K molecule contrasts with G0PS-P2VP5K copolymer, which does not gel even at 10 times higher concentrations ($\phi\sim0.1$). Our previous DLS [9,44] measurements showed that molecular expansion was found to be significantly larger for the arborescent polymers grafted with longer 30K polyelectrolyte chains, compared to 5K chains. The gelation for 30K sample may reflect this effect of expansion upon charging polymers. Increasing the ionization level ($\alpha>0.4$) caused a gel to change back to a liquid. For G0PS-P2VP30K system in methanol-$d4$, $\alpha=0.4$ is the transition point where the effective charge starts to decrease with increasing acid concentration due to charge renormalization. The large contraction of charged 30K chains induced by charge renormalization was previously observed [44]. As a result, a gel weakens and the liquid state is recovered for $\alpha>0.4$. The SANS data for G0PS-P2VP30K polymer solutions at fixed concentration ($\phi=0.01$) are provided in Fig. 7(a). Upon gelation the scattering intensity decreases due to the increase of total osmotic pressure upon addition of HCl. The interesting feature in SANS data collected for a gel is the appearance of broad shoulders at higher q in addition to the interparticle correlation peak in lower q. The primary peak appeared in the SANS for a gel is sharper than that for liquid state and the higher q shoulders are found only for a gel. These indicate that charged copolymers in a gel are less randomly distributed than in liquid state. This type of broad shoulders in addition to the primary peak in small-angle scattering curves has often been observed for microphase separated block copolymer systems and interpreted as the evidence of liquid-like ordering of

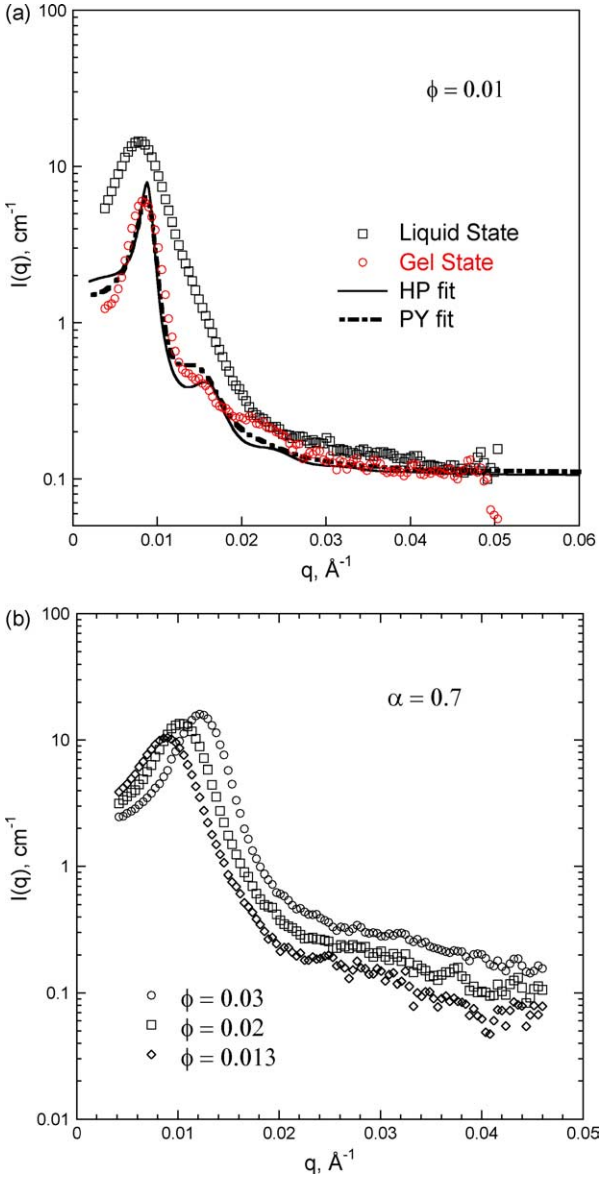

Fig. 7. SANS of G0PS-P2VP30K in methanol-*d*4 (a) Comparison of liquid state (slightly charged $a<0.001$) and gel state ($a=0.3$) for same solution concentration ($f=0.01$), The HP and PY (percus-Yevick) model fits to the data from a gel (b) Screened gel (Liquid state, $a=0.7$) as a function of f.

spherical micelles [45–47]. The liquid-like ordering of these non-charged solutions has been quantitatively analyzed by the Percus–Yevick model for small-angle scattering data analysis [48]. The Percus–Yevick approximation delineates hard sphere (excluded volume) interactions and has been successfully applied to many high density fluids and liquid state systems [45–47]. The gelation of G0PS-P2VP30K copolymers appears to be attributed to not only long-range Coulombic interactions but also the increased packing density of significantly expanded polyelectrolyte branch. It is then possible to assume that unlike 5K charged solutions, a gel may resemble the behavior of highly concentrated fluids where liquid-like ordering occurs principally due to hard sphere interactions. Both the Percus–Yevick and Hayter–Penfold models for $S(q)$ using the hard sphere model for $P(q)$ were fit to the experimental data from a gel. The polydisperse $S(q)$ for hard

Table 5
Structural parameters determined by fittings of SANS data for the gel

	R_h (Å)	Polydispersity[a]	Volume fraction (η)	Charge (z)
HP model	386	0.22	0.5	20
PY model	376	0.15	0.55	–

[a] The polydispersity $=\sigma/R_h$ where σ^2 is the variance of the distribution.

sphere interactions by the Percus–Yevick approximation was derived by Griffith et al. [49]. A large increase in the molecular size for a fitting parameter is necessary to fit the data, particularly the second shoulder in the higher q regime indicating that the shoulders originates from the form factor of substantially expanded G0PS-P2VP30K polymers. The structural parameters obtained from both fits are summarized in Table 5. Although both model fits give relatively a good agreement with the primary peak, the deviation with the experimental data becomes larger in the higher q regime. The deviation may be reduced by using a more appropriate model, which takes into account the combined effects of charge and hard sphere interactions for this polyelectrolyte gel system. As the solution changes from a gel to a liquid, the shoulders in higher q disappeared [Fig. 7(b)] reflecting the substantial contraction of 30K P2VP chains due to the screening of electrostatic interactions as previously observed by DLS [44]. The peak position scales with polymer concentration [Fig. 7(b)] according to $q^*=k\phi^n$ with $n=0.34\pm0.03$ molecules. In contrast to low α ($=0.2$), for higher α ($=0.7$) arborescent polymers do not interpenetrate in a manner sufficient to induce gelation even at $\phi>\phi^*$ (~0.01) where ϕ^* is the overlap concentration (gelation begins) for lower α values. This is consistent with the theoretical prediction for highly branched polyelectrolyte solutions that the system should be self-screened with the molecules being impenetrable and exhibiting liquid-like ordering at $\phi>\phi^*$ [42].

4. Conclusions

The combined investigation of SANS with DLS were carried out on the dilute solutions of charged arborescent G1, polystyrene-*graft*-poly(2-vinylpyridine) copolymer. The SANS curves from charged G0PS-P2VP5K copolymers in methanol-*d*4 and D_2O displayed an interference peak. The calculation of the interparticle distance for a uniform particle distribution and a comparison to the values from the experimental data ($d_{exp}\cong d_{uni}$) indicates that the scattering peak represents the liquid-like ordering of charged arborescent graft polymers due to long-range Coulombic intermolecular repulsions. The Hayter–Penfold model for $S(q)$ was used to fit the SANS data for charged G0PS-P2VP5K copolymer in solutions. The number of effective charge obtained from the fits by the Hayter–Penfold model was consistent with the trend of the peak evolution as a function of charge density, indicating that charged arborescent polymers may interact via the screened repulsions which are qualitatively similar to the DLVO potential. The smaller dielectric constant of methanol-*d*4 resulted in long-range electrostatic repulsions persisting to lower polymer concentration than in D_2O. The dynamic light

scattering showed two diffusive relaxations processing upon addition of HCl to the G0PS-P2VP5K polymer solution. The slow mode dynamics observed by DLS possibly indicates the local structural inhomogeneity of arborescent graft polyelectrolyte solutions. The peak and slow mode disappeared simultaneously due to the screening of electrostatic interactions upon addition of excess HCl into solutions. The molecular expansion was found to be more significant for the polymer with longer polyelectrolyte branch chains (P2VP30K) than shorter ones (P2VP5K), which resulted in the P2VP30K molecules forming a gel upon addition of acid at low acid concentrations ($0<\alpha<0.4$). The gel breaks on the further acid addition ($\alpha>0.4$) resulted from the screening by the counterions drawn into the intermolecular volume.

Acknowledgements

This work has benefited from the use of the 30 m NIST-NG3 and NIST-NG7 instruments at the Center for Neutron Research at the National Institute of Standards and Technology. We acknowledge the support of the National Institute of Standards and Technology, US Department of Commerce, for its providing the neutron research facilities used in this experiment. The authors thank Dr S. Kline at NIST for his assistance with SANS experiments and data analysis. The authors also thank Dr O. Wilson at University of Maryland at College Park for his help with DLS experiments and data analysis. R.A. Kee and M. Gauthier thank the Natural Sciences and Engineering Research Council of Canada for the financial support.

References

[1] Teertstra SJ, Gauthier M. Prog Polym Sci 2004;29:277.
[2] Voit B. J Polym Sci, Part A: Polym Chem 2000;38:2505.
[3] Matthews OA, Shipway AN, Stoddart JF. Prog Polym Sci 1998;23:1.
[4] Wiesler UM, Weil T, Müllen K. Top Curr Chem 2001;212:1.
[5] Tomalia DA. Aldrichimica Acta 2004;37:39.
[6] Konar N, Nujoma Y, Kim C. In: Tripathy SK et al, editor. Handbook of polyelectrolytes and their applications of polyelectrolytes and theoretical models, vol. 3. Stenvenson Ranch, CA: American Scientific Publishers; 2002. p. 47.
[7] Shi X, Shen M, Möhwald H. Prog Polym Sci 2004;29:987.
[8] Kee RA, Gauthier M. Macromolecules 2002;35:6526.
[9] Gauthier M, Li JM, Dockendorff J. Macromolecules 2003;36:2642.
[10] Briber RM, Bauer BJ, Hammouda B, Tomalia D. Abstr Pap Am Chem Soc 1992;204:225.
[11] Nisato G, Ivkov R, Amis EJ. Macromolecules 1999;32:5895.
[12] Ohshima A, Konishi T, Yamanaka J, Ise N. Phys Rev E 2001;64: 051808.
[13] Ramzi A, Scherrenberg R, Joosten J, Lemstra P, Mortensen K. Macromolecules 2002;35:827.
[14] Schmitz KS, Lu M, Gauntt J. J Chem Phys 1983;78:5059.
[15] Valachovic DE. Thesis. University of Southern California; 1997.
[16] Stigter D. Biopolymers 1979;18:3125.
[17] Förster S, Schmidt M, Antonietti M. Polymer 1990;31:781.
[18] Smits RG, Kuil ME, Mandel M. Macromolecules 1994;27:5599.
[19] Seldak M. J Chem Phys 1996;105:10123.
[20] Borsali R, Nguyen H, Pecora R. Macromolecules 1998;31:1548.
[21] Matsuoka H, Schwahn D, Ise N. Macromolecules 1991;24:4227.
[22] Sogami I, Ise N. J Chem Phys 1984;81:6320.
[23] Schmitz KS, Bhuiyan LB. Phys Rev E 2000;63:011503.
[24] Ise N, Okubo T, Yamamoto K, Kawai H, Hashimoto T, Fujimura M, et al. J Am Chem Soc 1980;102:7901.
[25] Ise N, Okubo T, Sugimura M, Ito K, Nolte HJ. J Chem Phys 1983;78:536.
[26] Gröhn F, Antonietti M. Macromolecules 2000;33:5938.
[27] Larsen AE, Grier DG. Nature (London) 1997;385:230.
[28] Yun SI, Briber RM, Kee RA, Gauthier M. Polymer 2003;44:6579.
[29] NG3 and NG7 30-meter SANS Instruments Data Acquisition Manual, National Institute of Standards and Technology Cold Neutron Research Facility; 1996.
[30] Glinka CJ, Barker JG, Hammouda B, Krueger SJ, Moyer JJ, Orts WJ. J Appl Crystallogr 1998;31:430.
[31] Rubinstein M, Colby RH. Polymer Physics. New York: Oxford University Press; 2003.
[32] Provencher SW. Comput Phys Commun 1982;27(213–227):229–42.
[33] Guenoun P, Delsanti M, Gazeau D, Mays JW, Cook DC, Tirrell M, et al. Eur Phys J B 1998;1:77.
[34] Matsuoka H, Ise H, Okubo T, Kunugi S, Tomiyama H, Yoshikawa Y. J Chem Phys 1985;83:378.
[35] Nisato G, Ivkov R, Amis EJ. Macromolecules 2000;33:4172.
[36] Boryu VY, Erukhimovich IYa. Macromolecules 1988;21:3240.
[37] Shibayama M, Tanaka TJ. Chem Phys 1995;102:9392.
[38] Ermi BD, Amis EJ. Macromolecules 1998;31:7378.
[39] Roij R van, Dijkstra M, Hansen J-P. Phys Rev E 1999;59:2010.
[40] Hayter JB, Penfold J. Mol Phys 1981;42:109.
[41] Alexander S, Chaikin PM, Grant P, Morales GJ, Pincus P, Hone D. J Chem Phys 1984;80:5776.
[42] Borisov OV, Daoud M. Macromolecules 2001;34:8286.
[43] The term 'excess HCl' is used for α where the peak in SANS become less pronounced addition of HCl. Excess HCl is not necessarily 'stoichiometric excess HCl' where α is always larger than 1.
[44] Yun SI. PhD Thesis. College Park: University of Maryland; 2002.
[45] Kinning DJ, Thomas EL. Macromolecules 1984;17:1712.
[46] Kinning DJ, Thomas EL, Fetters LJ. J Chem Phys 1989;90:5806.
[47] Adams JL, Quiram DJ, Graessley WW, Register RA. Macromolecules 1996;29:2929.
[48] Percus JK, Yevick G. J Phys Rev 1958;110:1.
[49] Griffith WL, Triolo R, Compere AL. Phys Rev A 1987;35:2200.